2020 IEEE Conference on Control Technology and Applications (CCTA)
August 24-26, 2020. Montréal, Canada

Model-based MIMO isoflux plasma shape control at the EAST tokamak: experimental results

R. Ambrosino[1], A. Castaldo[2], G. De Tommasi[1], *Senior Member, IEEE*,
Z. P. Luo[3], Y. Huang[3], A. Mele[2], A. Pironti[1], Y. H. Wang[3], B. J. Xiao[3]

***Abstract*— This paper reports on the experimental validation of a MIMO plasma shape controller at the EAST tokamak, carried out during the 2019-2020 experimental campaign. In particular the decoupled SISO controller that is routinely used during operations at EAST, was temporarily replaced by a MIMO isoflux controller, whose design is based on the *eXtreme Shape Controller* approach, which permits to control a larger number of plasma shape parameters. The proposed plasma shape controller has proven to be able of withstanding relevant disturbances, i.e. to the additional power injections required to reach an almost fully non-inductive current driven regime.**

Keywords: plasma magnetic control, tokamak, model-based control, MIMO controller.

I. INTRODUCTION

Tokamaks are experimental fusion devices aimed at proving the feasibility of energy production by means of nuclear fusion. In a tokamak, a plasma (a fully ionized gas) of hydrogen ions, is confined by magnetic fields and heated to temperatures of the order of hundreds millions of degrees. The plasma confinement is achieved by means of a set of external coils wrapped around the vacuum vessel, that produces the toroidal magnetic field (see Fig. 1). An additional external field is produced by a set of toroidal coils, called *Poloidal Field* (PF) coils. Such an additional magnetic field is needed to induce current into the plasma itself, and to change its shape and position.

Reliable and robust operations of modern tokamaks call for active control of the poloidal component of the magnetic field. The main objectives of magnetic control are the regulation of the plasma current and shape, as well as the vertical stabilization. For a complete overview of magnetic control in tokamaks, the reader is referred to [1], [2]. Here we just mention the main reasons that call for an effective plasma shape control in a tokamak. Indeed, the control of the shape of the plasma poloidal cross-section (see the magenta curve in Fig. 2) is essential, since the plasma has to occupy as much volume as possible within the vacuum chamber. This means that the distance between the plasma boundary and the facing metallic structures should be kept small. On top of that, during tokamak operation, high-energy

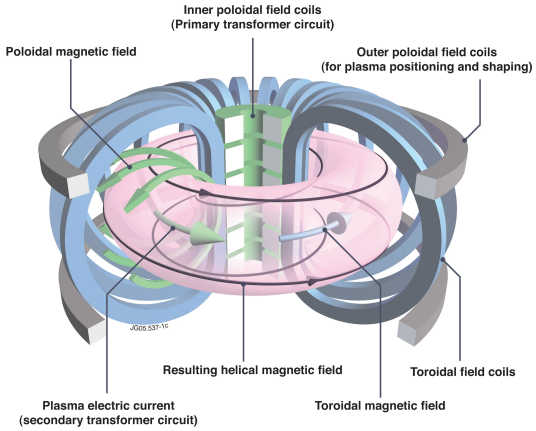

Fig. 1. Simplified scheme of a tokamak reactor.

ionised particles are produced and leave the plasma after the confinement time [3]; all these ionised particles must be removed and collected by the divertor structure. Plasma shape control represents an effective tool to reduce the thermal load on the divertor structures, either by performing a periodic movement of the strike-points, the so called *strike-point sweeping* [4], or by reaching advanced magnetic configurations in the *scrape-off-layer* region [5].

In this work the results obtained at the EAST tokamak during the 2019-2020 experimental campaign are presented. The experiments that were carried out aimed at improving the capabilities of the EAST plasma shape control system. Indeed, a set of SISO controllers is routinely used during operations at EAST [6], where each loop controls the plasma shape error along one of the segments shown in Fig. 2, by driving the current in a set of dedicated PF coils. This solution was replaced by a MIMO isoflux controller, whose design is based on the *eXtreme Shape Controller* (XSC) approach, which was originally proposed at the JET tokamak for plasma *gap-based* shape control [7], [8], and which was also used for the control of plasma internal profiles on other devices (as an example see [9]). The XSC approach permits to control a larger number of plasma shape parameters compared to the SISO solution, by minimizing, at steady-state, the plasma shape error in the least mean square sense [10]. The paper is structured as follows: in the next section the plasma shape control problem (sometimes also referred to as plasma *boundary* control) is recalled; this section also introduces the linear model exploited in Section III to design

[1]R. Ambrosino, G. De Tommasi and A. Pironti are with Dipartimento di Ingegneria Elettrica e delle Tecnologie dell'Informazione, Università degli Studi di Napoli Federico II and with Consorzio CREATE, via Claudio 21, 80125 Napoli, Italy.

[2]A. Castaldo and A. Mele are with Consorzio CREATE, via Claudio 21, 80125, Napoli, Italy.

[3] Z. P. Luo, Y. Huang, Y. H. Wang and B. J. Xiao are with Institute of Plasma Physics, Chinese Academy of Sciences, Hefei 230031, People's Republic of China.

Authorized licensed use limited to: Auckland University of Technology. Downloaded on November 03,2020 at 23:31:41 UTC from IEEE Xplore. Restrictions apply.

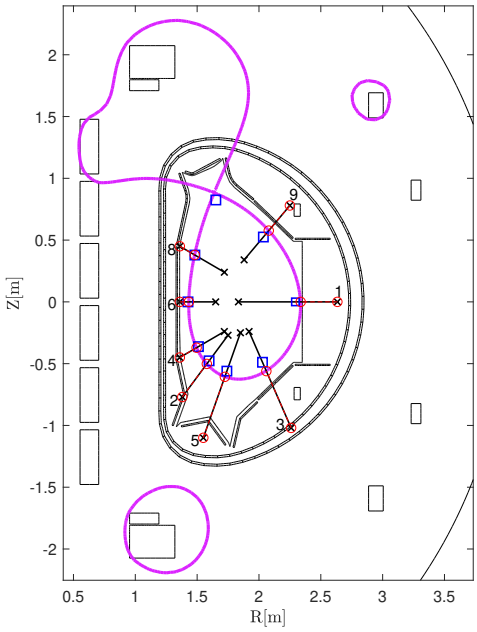

Fig. 2. Poloidal cross-section of the EAST tokamak. The plasma shape, i.e. the Last Closed Flux Surface (LCFS), for the pulse #92686 at the flattop is also reported. The control segments considered by the proposed plasma shape controller are also shown, as well as the shape reference points, including the desired X-point location (blue squares).

the proposed MIMO *isoflux* plasma shape controller. The main contribution of this paper is given in Section IV, where the results achieved at EAST show that the proposed approach permits to control the plasma shape in presence of relevant disturbances, i.e. when the additional heating power is such that an almost fully non-inductive current driven regime is achieved. Some conclusive remarks and future perspectives are eventually discussed in Section V.

II. PLASMA SHAPE CONTROL IN TOKAMAK FUSION REACTORS

In this section we briefly introduce the plasma shape control problem as well as a linear model that describes the behaviour of the plasma column and of the currents flowing in the surrounding coils. This model is used for the design of plasma shape controller in Section III.

A. Plasma electromagnetic modelling

As far as the so-called magnetic control in tokamak is concerned, the behavior of the plasma and of the currents in the surrounding conductive strcutures can be modeled resorting to some simplifying assumptions, such as the axisymmetry of the device and the absence of dissipative effects (e.g. resistivity and viscosity). Moreover, the plasma is usually assumed to evolve in a quasi-static fashion through a series of equilibrium states whose magnetic topology consists, inside the plasma, of a set of nested magnetic surfaces. Each of these equilibria can be described by a single elliptic nonlinear PDE known as the Grad-Shafranov equation [11], which can be written in cylindrical coordinates (r, z, φ) as

$$\Delta^* \psi = -\mu_0 r J_\varphi \left(r, z, \psi\right) , \tag{1}$$

where ψ is the magnetic flux across a circle passing at (r, z) expressed in Wb/rad, μ_0 is the vacuum permeability, J_φ is the toroidal current density, which in general depends both on the coordinates (r, z) and on the solution to the problem ψ, and Δ^* is an elliptic differential operator given by

$$\Delta^* = r \frac{\partial}{\partial r} \left(\frac{1}{r} \frac{\partial}{\partial r} \right) + \frac{\partial^2}{\partial z^2} .$$

This equation can be coupled to the dynamics of the surrounding circuits (PF coils and passive structures essentially), which can be simply expressed through Kirchhoff equations. The main complication is that of computing the mutual inductance between the plasma (treated as a deformable conductor) and said circuits. The dissipative effects in the plasma can be re-introduced a posteriori, by selecting an appropriate resistance value for it (more on this point in the following). Moreover, for control purposes the dynamic response of the plasma can be linearized in the surroundings of a chosen reference equilibrium, which describes a desired configuration. This is what is done in the CREATE equilibrium codes [12] that solve the Grad-Shafranov equation (1) and generate linearized models of the plasma response around the considered MHD equilibrium. These models can be put in a standard state-space form

$$\delta \dot{x}(t) = A\delta x(t) + B\delta u(t) + E\delta \dot{w}(t) \tag{2a}$$

$$\delta y(t) = C\delta x(t) + D\delta u(t) + F\delta w(t) , \tag{2b}$$

where:

- A, B, C, D are standard state-space matrices;
- $\delta x(t)$ is the state vector, which contains the variations of the currents in the active circuits, in the passive structures, and the plasma current;
- $\delta u(t)$ is the input vector, which contains the voltages variations applied to the considered active circuits;
- $\delta y(t)$ is a vector containing the outputs variations; the outputs we are interested in are mainly the plasma current and quantities related to the plasma magnetic geometry. The latter include position and flux of both plasma centroid and active X-point, simulated magnetic measurements (in terms poloidal flux and magnetic field) evaluated at different points of the vacuum chamber, plasma-wall gaps, and so on;
- $\delta w(t)$ contains the β_p and l_i profile parameters variations. These two parameters describe the plasma internal distribution of pressure and current, respectively, and they can be considered as external disturbances from the point of view of the magnetic control system. The E and F matrix quantify their effect on the system dynamics.

The described model can be used for controller synthesis, as it will be discussed in section III.

Authorized licensed use limited to: Auckland University of Technology. Downloaded on November 03,2020 at 23:31:41 UTC from IEEE Xplore. Restrictions apply.

B. Plasma magnetic control

The main tasks to be achieved by any plasma magnetic control system are the following.

- **Plasma current control**, that is to regulate the current flowing in the plasma to a desired value and feedback is needed, since the plasma resistivity may not accurately compensated by the feedforward and the plasma current may be influenced by external current drive systems, whose effect is difficult to estimate *a priori*. In particular, high levels of injected powers may lead to *non-inductive* discharges, where the plasma current is no longer sustained by the transformer current, but is instead generated by means of external current drive sources or by a physical mechanism known as *bootstrap current*.
- **Vertical Stabilization**, i.e. to stabilize the plasma position in the vertical direction (more details can be found in [13]).
- **Shape control**: achieving a desired magnetic geometry, in particular for what concerns the Last Closed Flux Surface (LCFS).

As far as plasma shape control is concerned, this is often used to obtain particular magnetic configurations which allow to achieve specific goals such as improved fusion performances, a better exploitation of the available space or a better distribution of the heat exhaust on dedicated machine structures [5]. Of course, due to the harsh conditions inside a fusion reactor, the magnetic field/flux near the plasma cannot be measured directly. The magnetic configuration is instead reconstructed by means of dedicated codes which exploits external magnetic sensors and solve the Grad-Shafranov equation (1) online. This task becomes particularly hard when the plasma current is very low and the eddy currents induced in the passive structures are significant, as in the first phases of a tokamak discharge. For this reason, in such phases often a simpler control logic is used, aimed at controlling only the plasma centroid position, which can be directly estimated from the magnetic measurements without need for a dedicated reconstruction code. The combination of centroid position and plasma current control is often referred to as *RZIP* control.

On the other hand, in most cases proper shape control is dealt with by means of one of two possible approaches: *isoflux* control or *gap* control.

III. MIMO ISOFLUX SHAPE CONTROL AT EAST

In the previous section we gave an overview of the possible approaches to control the shape of the plasma columns inside the vacuum chamber of a tokamak fusion reactor. We now focus on the MIMO isoflux approach that has been implemented within the EAST Plasma Control System (PCS, [6]), with the aim of effectively controlling advanced magnetic configurations [5]. The proposed approach extends to the isoflux case the one used for the XSC at the JET tokamak.

From equation (2b), it can be seen how the relation between the n_{PF} active currents and the outputs (in our case chosen as a set of n_G plasma shape descriptors) is essentially static. This comes from the assumption that the plasma evolution happens through a set of equilibria, i.e. a change in the currents (whose behaviour contains the models dynamics) is immediately visible on the plasma configuration (which is assumed to be an algebraic function of the state variables, as internal plasma dynamics are assumed to be negligible due to their much faster time scale). Neglecting the external disturbances and assuming $D = 0$ (an assumption that is always satisfied in practice), this relation can be rewritten in the form

$$\delta\mathbf{Y}(s) = \bar{C}\delta\mathbf{I}_{PF}(s)\,,$$

where the vector $\delta\mathbf{Y}(s)$ are the deviation of the considered outputs from the equilibrium value, while $\bar{C}$ denotes the $n_G \times n_{PF}$ part of the C matrix which links the considered state and output variables. When isoflux plasma shape control is considered, the output vector $\delta\mathbf{Y}$ includes the $(r\,, z)$ coordinates of the X-point, the magnetic field at the X-point, and the poloidal flux differences $\Delta\psi$ at the control points shown in Fig. 2.

Suitable PFC current references can be computed by the shape controller and added to the preprogrammed scenario currents and to the contributes of other control loops (i.e. the plasma current controller) via the relation

$$\delta\mathbf{I}_{PF_{ref}} = \bar{C}^{\dagger}\delta\mathbf{Y}\,,$$

where $\bar{C}^{\dagger}$ denotes the pseudo-inverse of $\bar{C}$. This pseudo-inverse matrix can be computed via a (possibly truncated) SVD procedure. Moreover, the pseudoinversion can be applied to an opportunely weighted $\tilde{C}$ matrix to favor a more accurate control of some of the shape descriptors or the usage of some of the actuators, i.e. $\tilde{C} = Q\bar{C}R$. With this approach, up to n_{PF} linear combinations of shape descriptors can be controlled exactly. However, in principle the number of these descriptors might be larger than the number of available actuators, i.e. $n_G > n_{PF}$. In such case, it can be shown that the controlling to zero the error on the n_{PF} linear combinations $\bar{C}^{\dagger}\delta Y$ is equivalent to minimizing the steady-state performance index [10]

$$J_{XSC} = \lim_{t\to+\infty}(\delta\mathbf{Y}_{ref} - \delta\mathbf{Y}(t))^T Q^T Q(\delta\mathbf{Y}_{ref} - \delta\mathbf{Y}(t))\,, \tag{3}$$

where $\delta\mathbf{Y}_{ref}$ are constant references for the geometrical descriptors. The performance index (3) reduces to the least square error when Q is the identity matrix.

Finally, a set of n_{PF} dynamic regulators (for instance PID controllers) can be added.

To test the proposed control solution before the experiments, a dedicated simulation suite has been developed (for more details the interested reader may refer to [14]). In Figs. 3-4 the results obtained with a purely proportional controller with $K_P = 0.5$ and two PI controllers with $K_P = 0.25\,, K_I = 1.25$ and $K_P = 0.25\,, K_I = 2.50$ are shown. It can be seen that the simulation tools allow to reliably reproduce the experiment, hence have been exploited to optimize the PI gains offline. In particular,

Authorized licensed use limited to: Auckland University of Technology. Downloaded on November 03,2020 at 23:31:41 UTC from IEEE Xplore. Restrictions apply.

the tuning has been carried with the aim of improving the control in the case of a relevant variation of β_p, i.e. an increase similar to the ones that typically occur when about 1 MW of additional heating is used to achieve an almost fully non-inductive regime.

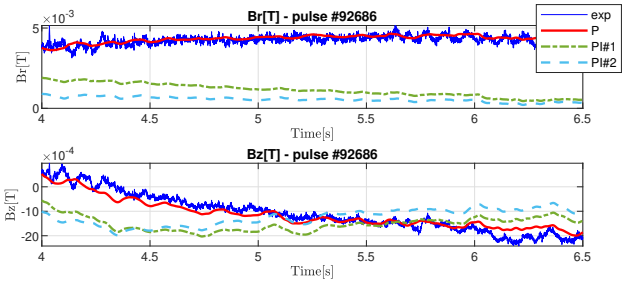

Fig. 3. Experimental and simulated magnetic field at the X-point target location. The blue trace shows the experimental values for the EAST pulse #92686, during which a proportional controller with $K_P = 0.5$ was used. The solid red trace the simulated signals, the dash-dotted green trace the results obtained in simulation with a PI controller with gains $K_P = 0.25\,, K_I = 1.25$ and the dashed cyan trace the ones obtained with a PI with gains $K_P = 0.25\,, K_I = 2.50$.

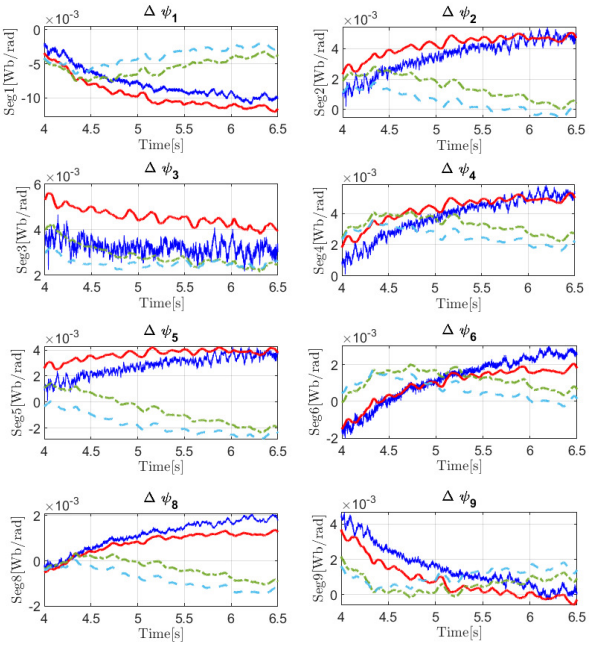

Fig. 4. Experimental and simulated magnetic flux errors at a set of target locations. The blue trace shows the experimental values for EAST pulse #92686, during which a proportional controller with $K_P = 0.5$ was used. The solid red trace the simulated signals, the dash-dotted green trace the results obtained in simulation with a PI controller with gains $K_P = 0.25\,, K_I = 1.25$ and the dashed cyan trace the ones obtained with a PI with parameters $K_P = 0.25\,, K_I = 2.50$.

IV. EXPERIMENTAL RESULTS

This section reports on the results obtained at EAST during the 2019-2020 experimental campaign. A number of experiments have been carried out with a twofold objective, that is to confirm the results obtained in simulation, and to assess the capabilities of the proposed controller in presence of relevant disturbances, i.e. of the foreseen power injection for fully current-driven scenarios. All the experiments considered in this section aims at controlling the plasma shape to the upper single-null configuration[1] shown in Fig. 2.

Figs. 5 and 6 show a comparison between pulses #92686 and #92719, aiming at confirming experimentally the tuning of the controller performed in simulation, as described in the previous section. In pulse #92686 the controller was purely proportional with $K_P = 0.5$, while in #92719 a PI controller with $K_P = 0.25$ and $K_I = 2.5$ was used. The first experiment, with an injected power of about 700 kW, shows a large steady-state error; to this purpose simulations suggested that the introduction of an integral action could be beneficial. This is indeed what can be seen in pulse #92719, where the error approaches much smaller values at regime for almost all of the controlled variables[2]. In the second case, in order to test the new controller, a smaller amount of power (about 400 kW) was injected in the plasma, resulting in a lower value of β_p and a slightly higher average plasma loop voltage V_{loop}. The noisier behaviour of the plasma, in this case, was probably due to impurities in the chamber: indeed, it can be seen how the same controller leads to much cleaner dynamics in the following experiments (Fig. 7 and 8). It is also worth to mention that, in all of the experiments shown here, the controlled variables for the X-point were the radial and vertical magnetic field components (B_r, B_z) at the target location; the position of the X-point has been reconstructed and is shown in the figures for completeness.

Figs. 7 and 8 show instead the results for pulses #92720 and #92723. In these experiments, both the available Lower-Hybrid (LH) launchers were used, hence a much higher level of power was injected in the plasma, in order to achieve an almost fully non-inductive current-drive regime. To this aim, differently from the previous cases, a second LH antenna was switched on at $t = 4s$, to inject up to 1 MW of heating power, resulting in the steep increase of β_p which can be observed in the Fig. 8, which acts as a disturbance on plasma shape control. More precisely, the disturbance entering the system is related to the β_p time derivative, hence a significant bump on all the controlled variables can be observed, which is well recovered by the controller in about 1 s. Moreover, the level of LH power injected in the plasma during pulse #92723 is enough to achieve the desired fully non-inductive regime, as confirmed by negative values reached by the V_{loop} during the experiment (see Fig. 8).

V. CONCLUSIVE REMARKS

The validation of a MIMO isoflux plasma shape controller has been presented in this paper. The validation has been carried out at the EAST tokamak, during the 2019-2020

[1] *Upper single-null* refers to a plasma configuration that an upper X-point.

[2] It should be recalled that the XSC approach minimizes the performance index 3, i.e. it minimizes the root mean square error on the controlled variables.

Authorized licensed use limited to: Auckland University of Technology. Downloaded on November 03,2020 at 23:31:41 UTC from IEEE Xplore. Restrictions apply.

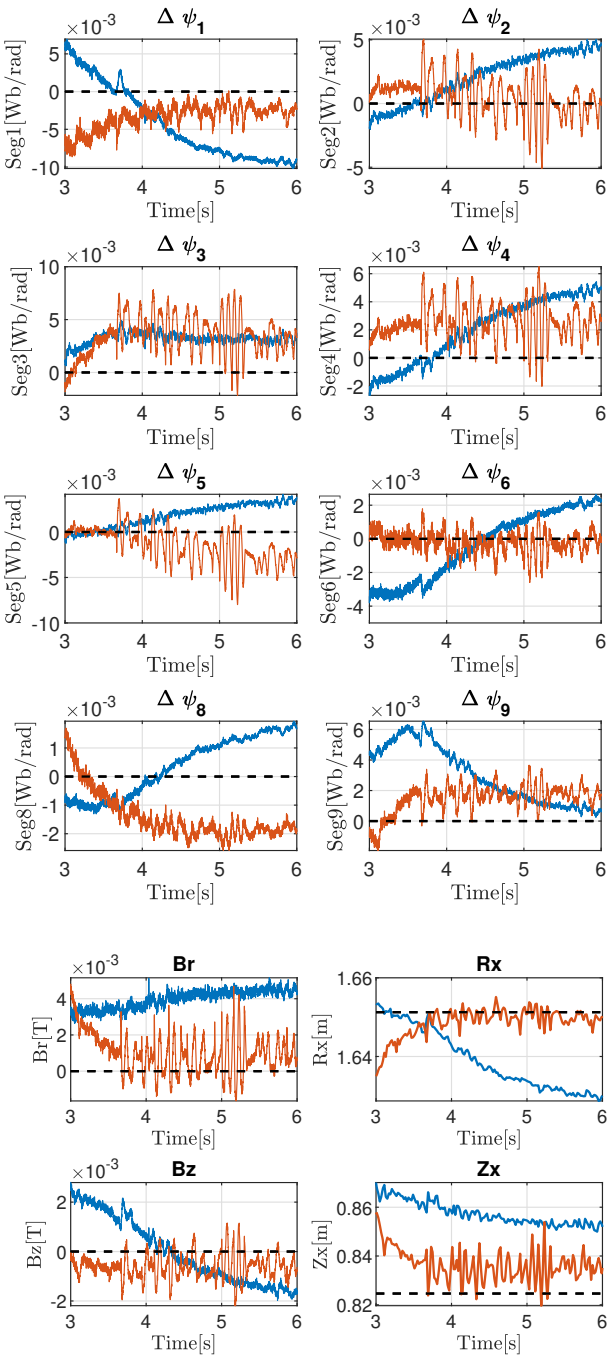

Fig. 5. Shape controller experimental results for pulses #92686 and #92719 (legend in the next figure).

experimental campaign. Experiments have confirmed the simulation results, and the proposed controller proved to be effective in rejecting the disturbances induced by the injection of additional heating power needed to reach fully non-inductive scenarios. These scenarios play an important role, since they represent the reference for long pulse operation, which are in turn envisaged in a fusion power plant. In order to improve usability of the proposed MIMO

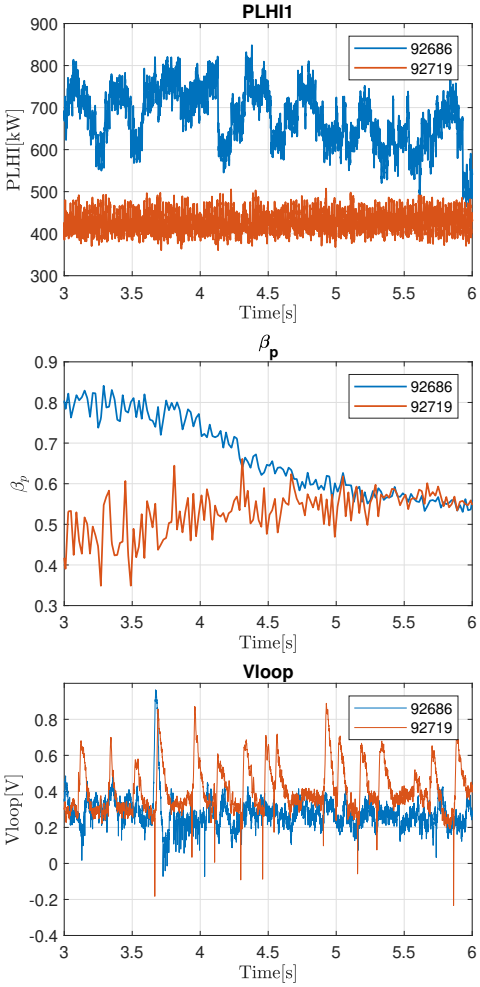

Fig. 6. Injected power, poloidal beta β_p and loop voltage for pulses #92686 and #92719.

approach, in future a gap-based version will be developed. Indeed, as mentioned in Section II-B, gap control provides a neater physical interpretation which can be exploited to increase the flexibility of the overall system [15].

ACKNOWLEDGEMENTS

This work has been carried out within the framework of the EUROfusion Consortium and has received funding from the Euratom research and training programme 2014-2018 and 2019-2020 under grant agreement No 633053. The views and opinions expressed herein do not necessarily reflect those of the European Commission.

This work was also partially supported by the Italian Research Ministry under the PRIN 20177BZMAH.

REFERENCES

[1] M. Ariola and A. Pironti, *Magnetic Control of Tokamak Plasmas*, 2nd ed. Springer, 2016.

[2] G. De Tommasi, "Plasma magnetic control in tokamak devices," *J. Fus. Energy*, vol. 38, no. 3-4, pp. 406–436, 2019.

[3] A. Loarte *et al.*, "Chapter 4: Power and particle control," *Nucl. Fus.*, vol. 47, no. 6, pp. S203–S263, 2007.

Authorized licensed use limited to: Auckland University of Technology. Downloaded on November 03,2020 at 23:31:41 UTC from IEEE Xplore. Restrictions apply.

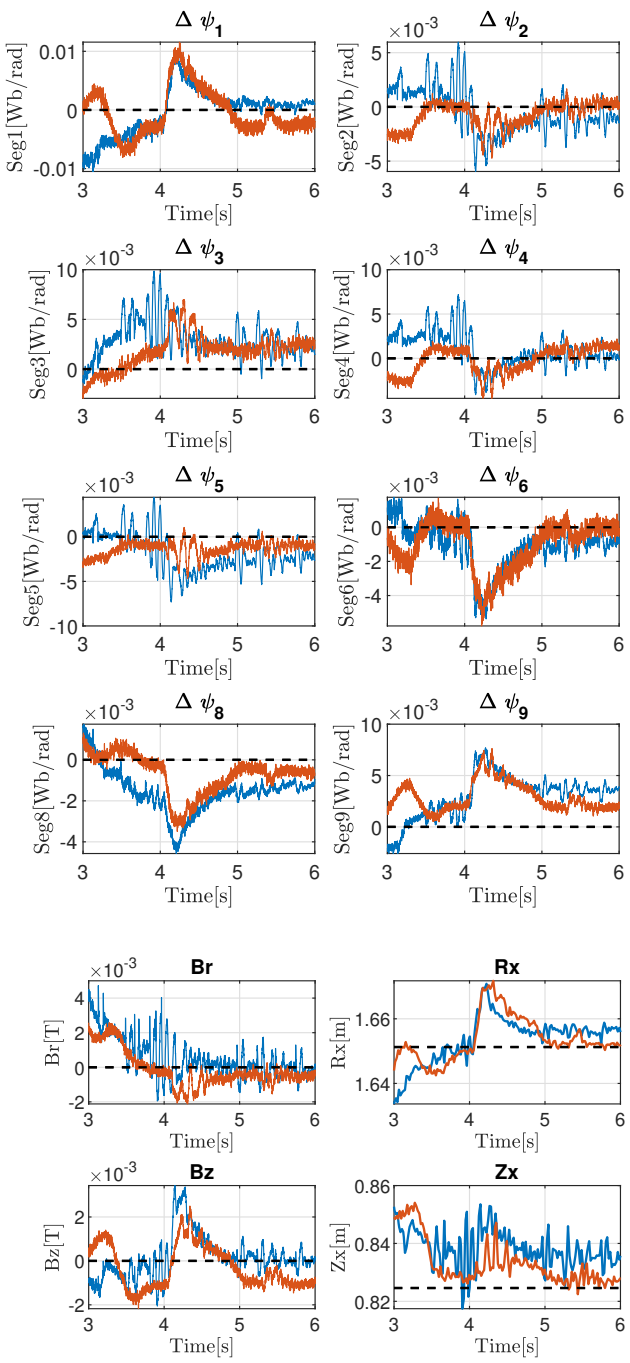

Fig. 7. Shape controller experimental results for pulses #92720 and #92723 (legend in the next figure).

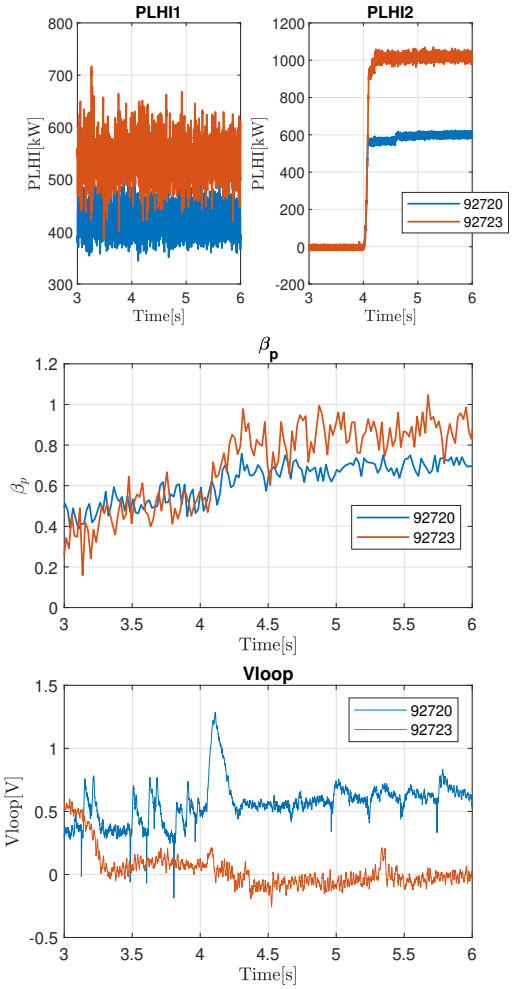

Fig. 8. Injected power, poloidal beta β_p and loop voltage for pulses #92720 and #92723.

pp. 65–75, 2005.

[8] G. Ambrosino, M. Ariola, A. Pironti, and F. Sartori, "Design and Implementation of an Output Regulation Controller for the JET Tokamak," *IEEE Trans. Control Syst. Technol.*, vol. 16, no. 6, pp. 1101–1111, 2008.

[9] W. Shi *et al.*, "A two-time-scale model-based combined magnetic and kinetic control system for advanced tokamak scenarios on DIII-D," in *Proc. IEEE Conf. on Decision and Control*, Maui, Hawaii, 2012, pp. 4347–4352.

[10] G. Ambrosino, M. Ariola, and A. Pironti, "Optimal steady-state control for linear non-right-invertible systems," *IET Control Theory & Applications*, vol. 1, no. 3, pp. 604–610, May 2007.

[11] J. Wesson and D. J. Campbell, *Tokamaks*. Oxford university press, 2011, vol. 149.

[12] R. Albanese, R. Ambrosino, and M. Mattei, "CREATE-NL+: A robust control-oriented free boundary dynamic plasma equilibrium solver," *Fus. Eng. Des.*, vol. 96-97, pp. 664–667, Oct. 2015.

[13] G. De Tommasi, A. Mele, Z. Luo, A. Pironti, and B. Xiao, "On plasma vertical stabilization at EAST tokamak," in *2017 IEEE Conference on Control Technology and Applications (CCTA)*, 2017, pp. 511–516.

[14] A. Castaldo *et al.*, "Simulation Suite for plasma magnetic control at EAST tokamak," *Fus. Eng. Des.*, vol. 133, pp. 19–31, 2018.

[15] G. De Tommasi *et al.*, "Shape control with the extreme shape controller during plasma current ramp-up and ramp-down at the jet tokamak," *J. Fus. Energy*, vol. 33, no. 2, pp. 149–157, 2014.

[4] G. Ambrosino *et al.*, "Plasma strike-point sweeping on JET tokamak with the eXtreme Shape Controller," *IEEE Trans. Plasma Sci.*, vol. 36, no. 3, pp. 834–840, 2008.

[5] G. Calabrò *et al.*, "EAST alternative magnetic configurations: modelling and first experiments," *Nucl. Fus.*, vol. 55, no. 8, p. 083005, 2015.

[6] Q. Yuan *et al.*, "Plasma current, position and shape feedback control on EAST," *Nucl. Fus.*, vol. 53, no. 4, p. 043009, 2013.

[7] M. Ariola and A. Pironti, "The design of the eXtreme Shape Controller for the JET tokamak," *IEEE Control Sys. Mag.*, vol. 25, no. 5,

Authorized licensed use limited to: Auckland University of Technology. Downloaded on November 03,2020 at 23:31:41 UTC from IEEE Xplore. Restrictions apply.